Supplementary Material

Supplementary Results

Hydrodynamics of dynacortin, N173 and C181

Dynacortin is an 80 kDa dimer with a large, 6 nm Stoke's radius (Robinson et al., 2002). Thus, dynacortin appears to be nonglobular, which is consistent with its high percentage of hydrophilic amino acid residues (Bairoch et al., 1997). We used platinum rotary shadowing and electron microscopy to view dynacortin, N173 and C181. Dynacortin appeared as elongated rods (Supplementary Figure 1A, B). Dynacortin particle size was 17 nm, which reduced to 15 nm after adjustment for platinum thickness (see Supplementary Methods; Supplementary Table 1). This is in close agreement with the Stoke's diameter (12 nm) determined from size exclusion chromatography (Supplementary Table 1). We then measured the hydrodynamic radius and the length of N173 and C181 (Supplementary Figure 1B; Supplementary Table 1). The lengths of each of these proteins after correction for platinum thickness were 6.1 nm and 7.9 nm, respectively.

Since C181 caused a downshift in the Stoke's radius of endogenous dynacortin when expressed in *D. discoideum* cells (Robinson and Spudich, 2000), we hypothesized that it might provide the dimerization domain. We analyzed N173 and C181 by sedimentation equilibrium centrifugation (Supplementary Figure 1C). The monomer molecular mass (MW) of His-N173 was calculated to be 20445.25 Da and by sedimentation analysis, N173 had a molecular mass of 20717 ± 389 Da (n=25) in salt ranging from 2-300 mM NaCl. Thus, N173 remains as monomers (Supplementary Table 1). For His-C181, the calculated MW was 21771.89 Da and by sedimentation analysis, the MWapp was 41212 ± 1600 Da (n=7). Thus, C181 forms dimers, providing the basis for dimerization of full-length dynacortin.

Analysis of the actin binding and cross-linking properties of N173 and C181

We examined and compared the actin binding and cross-linking properties of full-length dynacortin, N173 and C181, using co-sedimentation. N173 and C181 bound and cross-linked actin filaments (Supplementary Figure 2A). We used high-speed (100,000xg) sedimentation to measure total binding of protein to actin and low-speed (10,000xg) sedimentation to measure the formation of larger complexes of cross-linked actin. Because it is not necessary for saturation of the bundled complex to have the same stoichiometry as saturation of total actin, we first

determined the saturation ratios of dynacortin, N173 and C181 under both conditions (Supplementary Figure 2B). Dynacortin and C181 saturated actin at a ratio of two moles of protein per mole of actin under both conditions. Since dynacortin and C181 are dimers, this indicates a ratio of one dimer per actin. In contrast, N173 saturated actin at a ratio of one monomer per actin under both conditions.

Given the saturation stoichiometries of full-length dynacortin and each of the half molecules and since at least two actin filaments are required to form a bundle, we used the binding models in Supplementary Figure 2C to evaluate our binding data. We analyzed the formation of bound complexes and cross-linked complexes by mixing protein and actin together in duplicate reactions then sedimenting the samples under high-speed and low-speed in parallel. Holding the actin constant over a variety of concentrations, we varied the protein so that we examined a wide range of protein and actin concentrations. We calculated K_{D1app} ($(1/K_1)^{1/2}$) from the high-speed samples and calculated $1/K_1K_2$ from the low-speed samples. From these two numbers, we were able to calculate K_{D2app} ($1/K_2$). In Table 2, we present data for K_{D1app} using 5-μM actin. The data for K_{D2app} is from a wide variety of actin concentrations, ranging from 1-20 μM actin. Our analysis determined that K_{D1app} is dependent on the actin concentration, rising linearly with increasing concentration. K_{D2app}, in contrast, was not actin-concentration dependent. Although a simple chemical equilibrium is expected to be concentration independent, the results, in fact, make intuitive sense. In essence, the cross-linking protein serves to inhibit itself by sequestering away the actin filaments. Since actin is a polymer, a few cross-links can quickly bury actin filaments (and hence available binding sites for additional cross-linking proteins). The apparent affinity then declines with increasing actin concentrations. Once the cross-linkers bind to the first actin, they can cross-link the second actin so that K_{D2app} is actin-concentration independent. Across all of our experiments the initial binding affinities of dynacortin and N173 for actin are indistinguishable. In contrast, C181 always showed a 2-3 fold lower affinity for initial binding. Dynacortin and C181 had similar K_{D2app} values, indicating that their ability to form bundles once bound to actin filaments is more similar. N173 had a lower affinity for cross-link formation than either of the other two. The relative abilities to bind and cross-link actin is reflected by $1/K_1K_2$ (Main text Table 2).

Analysis of the actin bundling activities of dynacortin and its domains

To verify that dynacortin, N173, and C181 are cross-linking and bundling actin, we assembled the bundles, then negatively stained and examined them by transmission electron microscopy (Supplementary Figure 3A). Dynacortin formed large parallel bundles as was anticipated from prior experiments (Robinson et al., 2002). C181 assembled the actin filaments into bundles that were morphologically indistinguishable from those formed by full-length dynacortin. N173 formed small bundles and cross-linked meshworks at similar concentrations but required much higher concentrations to form parallel bundles, though they never reach the large sizes observed for dynacortin and C181 (data not shown).

For a more quantitative view of the ability of each proteins to bundle actin, we developed a simple quantitative assay using fluorescence microscopy (Supplementary Figure 3 B, C). The assay used 1-μM rhodamine-phalloidin stabilized actin filaments and varying concentrations of dynacortin, N173, and C181. To quantitate the dynacortin, N173, and C181 concentration dependency of bundle formation, the standard deviation of the pixel intensity was calculated using unmodified digital micrographs. This parameter gave the best representation of the images. The rationale is that for images where the actin filaments are unbundled, the actin filaments fill the field, giving a relatively even field of fluorescence. As the filaments become bundled, more pixels acquire a high level of signal while a substantially larger number of pixels yield no signal. This leads to a bimodal distribution of pixel intensities, which is reflected in the standard deviation of pixel intensity. We calculated the mean of these standard deviations from six or more fields for each protein concentration. Then, plotting the standard deviation of pixel intensity versus protein concentration leads to a quantitative representation of the bundling by each protein. From this assay, the concentration of dynacortin that produced the half-maximal bundling activity was 1 μM (0.5-μM dynacortin dimer). N173 and C181 had half-maximal concentrations of around 60 μM and 15 μM (7.5-μM dimer), respectively. Thus, N173 and C181 are poorer bundlers than dynacortin, though C181 has properties that are more similar overall to the full-length dynacortin.

For an independent analysis of actin cross-linking behavior, we used falling ball viscometry to assess the concentration dependence of actin cross-linking (Supplementary Figure 3D). None of the proteins increased the apparent viscosity at extremely low concentrations

above actin-alone controls. However, only 0.5-1 μM dynacortin was required to increase the viscosity of 24-μM actin gels. By increasing the concentration of dynacortin to 2 μM, the actin became bundled, resulting in a phase separation. This is due to the concentration of the actin into bundles, producing a heterogeneous solution with regions devoid of actin bundles and low viscosity and regions where the bead was obstructed by the actin bundle mass. The data were uninformative in this regime. Significantly higher C181 dimer concentrations (15 μM) were required to increase the viscosity of the gel, though the amount of increase (2-3 fold) before phase separation was smaller than for dynacortin. 50-60 μM N173 was required to increase the viscosity of the actin gel. Intriguingly, the viscosity was increased much more (20-fold) by N173 than for either the full-length or C181 domains. Though N173 appears to be a poorer bundler, it appears to be a good cross-linker at high concentrations. Notably, the [cross-linker]-dependency determined by falling ball viscometry (which uses 24-μM filamentous actin) and the [cross-linker]-dependency from the fluorescence bundle assay (1-μM filamentous actin) were in close agreement.

In summary, dynacortin is more effective at actin cross-linking than either N173 or C181. But, each half domain is capable of binding and bundling actin filaments. The equilibrium constants indicate that both N173 and C181 cross-link with similar thermodynamics that are only somewhat lower than full-length dynacortin. However, from the cross-linking and bundling assays, an activity order is indicated in which dynacortin > C181 > N173. Since N173 and C181 bound actin with similar thermodynamics, it is possible that N173 has faster on and off rates than C181 or dynacortin, allowing it to achieve similar overall thermodynamics of actin cross-linking. These differences in actin cross-linking have implications for how each domain may influence the viscoelastic properties of the cortex.

Supplementary Materials and Methods

Constructs and Strains

Dynacortin (dynacortin a.a. 1-354), N173 (dynacortin a.a. 1-172) and C181 (dynacortin a.a. 173-354) were expressed using the pET14b (Novagen) expression plasmid (Figure 1). Constructs were generated using polymerase chain reaction and subcloned into the *Nde* I and *Bam*H I sites. The resulting plasmid encodes a 6xHis tag, followed by a thrombin cleavage site

then the complete dynacortin derivative. Stop codons were introduced at the end of the dynacortin peptide so as not to include any additional amino acid residues.

Protein expression and purification

For expression, we engineered an expression strain using BLR cells (Novagen) and the helper plasmid (pRARE), which includes the LysS and tRNAs for rare Arg, Ile, and Leu codons that is included in the Rosetta (Novagen) *Escherichia coli* cells. This plasmid was isolated from the Rosetta cells and introduced into BLR cells. We named the resulting strain BLAREs (BLR:pRARE). The advantage of this strain is that it now includes the DE3 lysogen for IPTG inducible expression of the T7 polymerase, lysozyme activity, rare tRNAs to help with the *D. discoideum* codon usage bias, and the *RecA* mutation. This combination of features increased expression 6-7-fold for full-length dynacortin as compared to what we have observed using other *E. coli* expression strains.

To begin purification, cultures were grown to an optical density of 0.6 at 600 nm. Expression was induced with 0.4 mM IPTG and cells were allowed to express for four hours. Cells were harvested by centrifugation, washed with 10 mM Tris pH 7.5, and resuspended at a density of one liter of cell culture equivalent per 30 mls of lysis buffer. Lysis buffer included 20 mM NaCl, 10 mM Hepes pH 7.1, 1 mM EDTA, and 1mM EGTA and a cocktail of protease inhibitors including the following: 0.1 mM phenylmethylsulfonyl fluoride, 150 μM 1-chloro-3-tosamido-7-amino-2-heptanone, 80 μg/ml L-1-tosylamido-2-phenylethyl chloromethyl ketone, 1 mg/ml benzamidine, 100 μg/ml Nα-*p*-tosyl-L-arginine-methyl ester, and 5 μg/ml leupeptin. Cells were lysed by freeze-thaw in liquid N_2. Lysates were clarified by centrifugation at 34,000xg for 25 minutes followed by precipitation with 0.25% polyethylenimine. The polyethylenimine precipitates were removed by centrifugation and the supernatants were fractionated by the addition of solid ammonium sulfate to 45% saturation. Full-length dynacortin, N173 and C181 each precipitate with the addition of 45% ammonium sulfate, resulting in a huge enrichment of each protein. The ammonium sulfate precipitates were solubilized in no salt A buffer (10 mM Hepes pH 7.1) and filtered through a 0.2 μm syringe filter to prepare the proteins for subsequent chromatographic steps using a BioRad Duo-Flow fast phase liquid chromatography system.

Full-length dynacortin was further purified first by separation on a Sephacryl S300 size exclusion column (Amersham) using the following buffer: 200 mM NaCl, 10 mM Hepes pH 7.1. Dynacortin eluted from this column with a K_{av} of 0.25. Fractions were pooled, diluted two-fold with no salt A and separated with a 20-column volume linear salt gradient from 28% B to 40% B where buffer B is 1 M NaCl, 10 mM Hepes pH 7.1 on a mono S HR 5/5 column (Amersham). Pure fractions were pooled, diluted in no salt A, reapplied to the mono S HR 5/5 column and eluted with 50% buffer B to concentrate the protein. The concentrated protein was dialyzed overnight to 2 mM NaCl, 10 mM Hepes pH 7.1, 1 mM NaN_3. With the BLARE cells, we typically recover around 2 mg of purified dynacortin per liter of bacterial culture.

N173 was purified by separation on a homemade 12-ml SP-sepharose Fast Flow (Amersham) column. The protein was eluted with a 10-column volume 20% B to 40% B gradient. The purified N173 was pooled, diluted two-fold in no salt A and concentrated on a monoS HR 5/5 (Amersham) column similar to full-length dynacortin. The protein was dialyzed into the same dialysis buffer. 1-2 mg of purified N173 per liter of bacterial culture were recovered from this protocol.

C181 was purified by separation on the same 12-ml SP sepharose but eluting with a 0-40% B salt gradient. The protein was further purified and concentrated on a mono S HR 5/5 column using a 20%-45% B salt gradient. We recovered 25 mg of purified C181 per liter of cell culture.

Actin was purified from chicken skeletal muscle using the methods of Pardee and Spudich (Pardee and Spudich, 1982). G-actin was further purified using an S300 Sephacryl column equilibrated in G-actin column buffer (10 mM Tris pH 7.5, 0.3 mM $CaCl_2$, 0.1 mM EDTA, 0.7 mM ATP, 0.02% NaN_3).

Rotary shadowing electron microscopy

Dynacortin, N173 and C181 particles were diluted in buffer at 50-300 μg/ml. 50 μl of sample was further diluted with spectroscopy grade glycerol at a 50% final concentration and loaded into a nebulizer. Samples were sprayed onto freshly cleaved mica squares with a Dust-off (Falcon) air can and loaded onto a Denton DV-502A metal evaporator. Samples were rotary shadowed (1 rpm) at $4x10^{-7}$ torr with 3.7 mg of platinum (Pella). The replicas were then supported with 6 nm of evaporated carbon then floated off on a drop of distilled water. Replicas

were picked up with glow discharged 400 mesh copper grids and blot dried with #1 filter paper (Whatman). All grids were viewed and photographed on a Phillips CM-120 TEM, operating at 80 kV. The metal thickness was estimated using the following equation: $wt_{Pt} = (4\pi 2dt\rho(10^{-5}))/(\sin s)$ where wt_{Pt} is the weight of platinum that was ionized, d is the distance from the point source (7 cm in our experiments), t is the thickness in Å, ρ is the bulk density of Pt (21.45 g/cm^3), and s is the shadowing angle 8°. The average thickness, t, was calculated to be 1.25± 0.046 nm from n=5 experiments. 2t (2.5) nm was substracted from the mean particle size to get a more accurate estimate of protein size.

Sizing by size-exclusion chromatography

To measure the hydrodynamic radius of dynacortin, N173 and C181, the proteins were separated on a calibrated high resolution S200 10/30 HR size exclusion column (Amersham) equilibrated in 200 mM NaCl, 10 mM Hepes pH 7.1. The column was calibrated with blue dextran (2000 kDa, $K_{av} = 0$) to mark the void volume, thyroglobulin (669 kDa, Stoke's radius 8.5 nm, $K_{av} = 0.12$), ferritin (440 kDa, Stoke's radius 6.1 nm, $K_{av} = 0.27$), catalase (223 kDa, Stoke's radius 5.2 nm, $K_{av} = 0.39$), bovine serum albumin (67 kDa, Stokes radius 3.5 nm, $K_{av} = 0.47$), cytochrome c (12.4 kDa, Stoke's radius 1.7 nm, $K_{av} = 0.76$), and vitamin B12 (1.3 kDa, $K_{av} = 0.96$). The total volume ($K_{av} = 1.0$) was marked by the conductance change caused by the difference in salt concentration from input protein and the running buffer. From these standards, the K_{av} for each was plotted against their respective Stoke's radius, the resulting points were fit to a linear equation. The Stoke's radii of dynacortin, N173, and C181 were calculated from each protein's K_{av}.

Molecular weight determination by analytical ultracentrifugation

To determine the stoichiometry of the His-tagged N173 and C181, the protein was subjected to equilibrium sedimentation analysis using a Beckman Optima XL-I analytical ultracentrifuge (Beckman Instruments). We used the calculated mass from the primary sequence to determine the monomer molecular weights. We also examined each protein by matrix-assisted laser desorption ionization-time of flight mass spectroscopy (MALDI-TOF) using an Applied Biosystems Voyager DE-STR MALDI-TOF to confirm the calculated masses (Johns Hopkins School of Medicine Mass Spec. facility). The partial specific volumes for His-N173

and His-C181 were calculated to be 0.7056 ml/g and 0.7259 ml/g, respectively. The solvent density was calculated for different salt concentrations by summing the incremental density contributions of the constituents. All calculations including temperature corrections were made by Laue's methods (Laue et al., 1992). C181 was measured at 300 mM NaCl. N173 was measured using solvents containing 2 mM, 25 mM, 50 mM, 75 mM, 150 mM or 300 mM NaCl, or 0.5xF-buffer or 1xF-buffer (10xF-buffer: 500 mM KCl, 10 mM $MgCl_2$, 10 mM EGTA, 2 mM ATP, 10 mM DTT, 100 mM imidazole, pH 7). The NaCl buffers contained 10 mM Hepes, pH 7.1. Initial protein concentrations ranged from 7.5 to 40 μM protein. Protein concentration was monitored by absorption at 280 nm. Initial concentration readings were taken at 3000 rpm. The samples were centrifuged at 16000, 17000, and 18000 rpm for at least 26 hours, then scans were taken every 2 hours until the sample reached equilibrium. Absorption curves were integrated after equilibrium and compared to the integrated absorption of the initial scan at 3000 rpm. The fractional amount of protein in the cell after reaching equilibrium compared to the initial sample was 0.99 ± 0.02 (n= 35; mean ± SEM) for N173 and 0.99 ± 0.02 (n=15; mean ± SEM) for C181, verifying that the measured molecular weight accurately reflects the population of protein and that there is no significant loss due to precipitation during the centrifugation. The average MWapp was determined by fitting multiple data files to a single ideal species model. All fits were performed using the Microcal Origin software (Beckman Instruments).

Analysis of actin interactions

***In vitro* cosedimentation:** G-actin was allowed to polymerize at high concentrations for 30 min at 22ºC by the addition of 10x Mg-exchange buffer (3 mM EGTA, 2 mM $MgCl_2$, 10 mM Tris, pH 7.5) followed by 10x-polymerization buffer (500 mM KCl, 10 mM $MgCl_2$, 10 mM EGTA, 2 mM ATP, 10 mM DTT, 100 mM imidazole, pH 7) to a final concentration of 1x for each buffer. Both actin and His-dynacortin were centrifuged to remove any aggregates before the assays were performed. Actin and His-dynacortin, N173 or C181 were mixed to appropriate concentrations and the dialysis buffer matched to each protein was added to normalize the volume of buffer from the dynacortin-derived protein. The reactions contained a final concentration of 0.5x or 1x polymerization buffer. Samples were incubated for 1 hr at 22ºC and sedimented at 100,000xg (total actin binding) in a TL100 ultracentrifuge for 25 min or at 10,000xg (actin bundling) in a microfuge for 25 min. Each reaction was prepared in duplicate so that one sample was

sedimented to analyze total actin binding and one sample was sedimented to analyze bundle formation. Supernatant and pellet fractions were collected, resuspended to a final concentration of 1x Laemmli's sample buffer and equivalent amounts were loaded on 15% SDS-PAGE gels. Gels were stained in Coomassie Blue stain and destained in 10% acetic acid. Proteins were quantified using an AlphaImager densitometer (Alpha Innotech Corp.). The linear ranges for dynacortin, N173, C181 and actin concentrations were determined so only appropriate amounts at each concentration were loaded on the gel for accurate quantification.

Electron microscopy: Various concentrations of His-dynacortin, N173, and C181 and 1-μM F-actin were mixed in 1x polymerization buffer and incubated for approximately 1 hr. Carbon coated copper grids were incubated with the protein mixture for 2 min. The grids were washed one time in filtered water and then grids were incubated in two changes of 1% uranyl acetate with 0.04% tylose for one min. each. Grids were dried by blotting on #1 filter paper (Whatman). All grids were imaged using a Phillips CM-120 TEM, operating at 80 kV.

Fluorescence microscopy: To examine the formation of actin bundles by light microscopy, actin filaments were labeled at a 1:1 mole ratio with tetramethyl rhodamine-labeled phalloidin (Molecular Probes). Varying concentrations of dynacortin, N173, and C181 were mixed with 1-μM labeled actin filaments and viewed on a Zeiss Axiovert fluorescence microscope using a 40X oil (NA=1.4) objective and a 1X optivar. Images were acquired using IP Lab (Scanalytics). Multiple images were acquired for each sample. All images were acquired using identical exposure times, filters, etc. From digital images of the samples, the standard deviation of the fluorescence intensity was determined for the population of pixels from the micrograph using Adobe Photoshop (Adobe Systems, Inc.).

Falling Ball Viscometry: For falling-ball viscometry (MacLean-Fletcher and Pollard, 1980), we mixed 1 mg/ml G-actin with varying concentrations of dynacortin, N173 or C181. 10x-polymerization buffer was added to a final concentration of 1x. The samples were immediately drawn into microcapillary pipets (VWR), capped, and incubated at 25°C for 3-4 hr. The viscosity, η, is inversely proportional to the velocity of the ball and proportional to constant $c = mg/(\sin\Theta * 6\pi r)$, where m is the mass of the ball, g is gravity, r is the ball radius and Θ is the angle of the tube (50° in our experiments). We used water (η = 1 mPa•s) and glycerol (η = 1408 mPa•s) to determine c for our set up. c was determined each day using standards. The velocity of a 0.7-mm steel ball was measured as it fell through the standards, uncross-linked actin gels, or

cross-linked actin gels. The viscosity, η, of actin gels without cross-linker was measured each day so that the viscosity of the cross-linked gels could be measured relative to actin-alone controls. This allowed for temperature and prep-to-prep variations to be accounted for though these variations amounted to at most 20-30% percent differences in c.

Supplementary References

Bairoch, A., Bucher, P. and Hofmann, K. (1997) The PROSITE database, its status in 1997. *Nucl. Acids Res.*, **25**, 217-221.

Laue, T.M., Shah, B.D., Ridgeway, T.M. and Pelletier, S.L. (1992) Computer-aided interpretation of analytical sedimentation data for proteins. In Harding, S., Rowe, A. and Horton, J.C. (eds.), *Analytical Ultracentrifugation in Biochemistry and Polymer Science*. Royal Society of Chemistry, Cambridge.

MacLean-Fletcher, S.D. and Pollard, T.D. (1980) Viscometric analysis of the gelation of Acanthamoeba extracts and purification of two gelation factors. *J. Cell Biol.*, **85**, 414-428.

Pardee, J.D. and Spudich, J.A. (1982) Chapter 18: Purification of muscle actin. *Methods Cell Biol.*, **24**, 271-289.

Robinson, D.N., Ocon, S.S., Rock, R.S. and Spudich, J.A. (2002) Dynacortin is a novel actin bundling protein that localizes to dynamic actin structures. *J. Biol. Chem.*, **277**, 9088-9095.

Robinson, D.N. and Spudich, J.A. (2000) Dynacortin, a genetic link between equatorial contractility and global shape control discovered by library complementation of a Dictyostelium discoideum cytokinesis mutant. *J. Cell Biol.*, **150**, 823-838.

Supplementary Figure Legends

Supplementary Figure 1. Dynacortin forms 15 nm rods. A. The images are a gallery of transmission electron micrographs of platinum rotary shadowed dynacortin particle replicas. The scale bar is 20 nm and applies to all images. B. Histograms representing the size distribution of metal shadowed particles of dynacortin, N173 and C181. The means, standard errors and n values are included. The means reported here are the actual sizes of the particles before the correction for the thickness of the metal layer, which is listed in Table 1. C. Sedimentation equilibrium analytical ultracentrifugation of N173 and C181. These graphs are example absorbance traces after the protein reached equilibrium. The fits are evolved from a model of a single ideal species. The residuals from the fits are presented.

Supplementary Figure 2. N173 and C181 bind to actin filaments *in vitro*. A. Using high speed co-sedimentation, unbound (supernatant, S) and bound (pellet, P) fractions were separated and then analyzed by denaturing polyacrylamide gel electrophoresis. The respective concentration of each protein used in each reaction is indicated. The salt conditions were 0.5x polymerization buffer. Over 85% of the N173 and C181 were ultimately pelleted at the highest actin concentrations. B. Dynacortin, N173, and C181 saturably bind actin filaments under high-speed and low-speed conditions. 1-μM F-actin and 0.5x polymerization buffer were used for these experiments. All concentrations used in these experiments were for monomeric protein. Therefore, dynacortin and C181 saturated at approximately 2 moles of monomer (1 mole of dimer) per mole of actin. N173 saturated at one mole of monomer per mole of actin. C. Binding models for dynacortin, N173 and C181 were evolved by combining the hydrodynamic properties ascertained by analytical ultracentrifugation with the saturation stoichiometries determined from the co-sedimentation experiments. These models were used to assess the apparent affinities for each step of actin cross-linking. A= actin.

Supplementary Figure 3. Dynacortin is the best actin cross-linker whereas C181 and N173 require progressively higher concentrations for actin cross-linking, respectively. A. Transmission electron microscopy of actin filaments ± dynacortin, N173 and C181. The actin bundles were assembled from 2 μM-filamentous actin in 1x polymerization buffer in each case. Scale bar (200 nm) for the actin alone panel applies to all images. B. Dynacortin bundles actin

into large arrays in a concentration dependent manner. 1-μM filamentous actin is labeled with rhodamine phalloidin for visualization. The concentrations are for monomeric dynacortin. Dimeric concentrations then are half of the value indicated. Scale bar (10 μm) applies to all panels. C. Dynacortin and its C181 and N173 domains have a cross-linking activity order of Dynacortin>C181>N173. The plots show how the mean standard deviation varies as a function of cross-linker concentration. Each point is the average of typically 6 or more micrographs per protein concentration. D. Relative actin cross-linking activities were measured using falling ball viscometry. Actin-alone controls were measured each day and all viscosities were normalized to the actin-alone controls for a given day. The amounts of cross-linker required to increase the apparent viscosity of 1 mg/ml actin was similar to the amounts required to increase the amount of bundling in the fluorescence assay in B and C. For dynacortin, the actin was organized into extended bundles. This results in a phase shift, which produces a mixture of dense actin bundles and actin free buffer. The beads showed a variety of high and low velocities due to drag from the bundles or low viscosity from the actin depleted domains of the capillary tube. Ordinarily, one would not expect drag from actin bundles since they are typically much smaller than the scale of the ball. However, dynacortin organizes actin filaments into bundles that can reach diameters of 1-μm and extended networks that are on the scale of the 0.7 mm ball (Robinson et al., 2002). In fact, the large networks of actin bundles are visible by eye at the higher concentrations of dynacortin. The data from these concentration ranges are indicated as gray circles to reflect the observations but to indicate that these data points are not useful for quantitative comparison.

Supplementary Table 1. Summary of the hydrodynamic properties of dynacortin, N173, and C181

Protein	Length, Pt. Shadowing (nm)	Stoke's Diameter (nm)	Stoichiometry
Dynacortin	15	12	2
N173	6.1	7.2	1
C181	7.9	8.5	2

Supplementary Table 2. P-Values from One-Tailed Student's T-Tests for |μ*| at 10 rad/sec and 100 rad/sec

10 rad/sec

	cortl^{1151}:pLD1	wt:N173	cortl^{1151}:N173	wt:C181	cortl^{1151}:C181	wt:dyn	cortl^{1151}:dyn	cortl^{1151}:cort	wt:pLD1w/lat
wt:pLD1	0.016	0.251	0.022	0.385	0.313	0.030	0.076	0.120	<0.0001
cortl^{1151}:pLD1		0.003	0.390	0.024	0.018	0.001	0.002	0.004	<0.0001
wt:N173			0.003	0.421	0.493	0.085	0.157	0.226	<0.0001
cortl^{1151}:N173				0.033	0.025	0.0002	0.003	0.005	<0.0001
wt:C181					0.432	0.107	0.158	0.216	<0.0001
cortl^{1151}:C181						0.156	0.207	0.272	<0.0001
wt:dyn							0.476	0.385	<0.0001
cortl^{1151}:dyn								0.420	<0.0001
cortl^{1151}:cort									<0.0001

100 rad/sec

	cortl^{1151}:pLD1	wt:N173	cortl^{1151}:N173	wt:C181	cortl^{1151}:C181	wt:dyn	cortl^{1151}:dyn	cortl^{1151}:cort	wt:pLD1w/lat
wt:pLD1	0.050	0.055	0.469	0.100	0.144	0.045	0.020	0.163	<0.0001
cortl^{1151}:pLD1		0.002	0.090	0.010	0.016	0.002	0.001	0.015	<0.0001
wt:N173			0.140	0.430	0.482	0.400	0.158	0.396	<0.0001
cortl^{1151}:N173				0.155	0.203	0.111	0.045	0.235	<0.0001
wt:C181					0.428	0.488	0.243	0.359	<0.0001
cortl^{1151}:C181						0.405	0.191	0.433	<0.0001
wt:dyn							0.222	0.321	<0.0001
cortl^{1151}:dyn								0.138	<0.0001
cortl^{1151}:cort									<0.0001

White Boxes: P-values ≤ 0.05

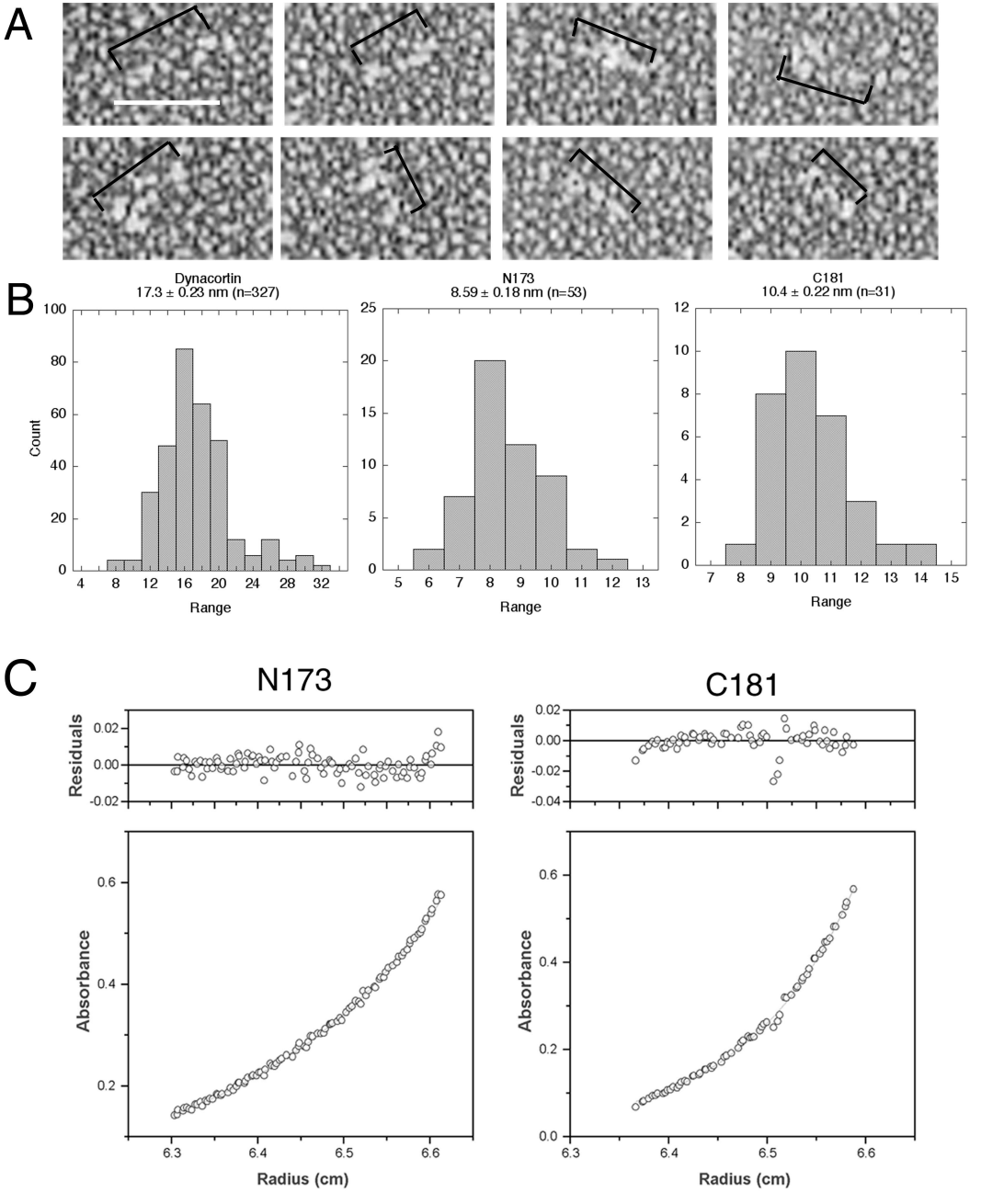

Supplementary Figure 1

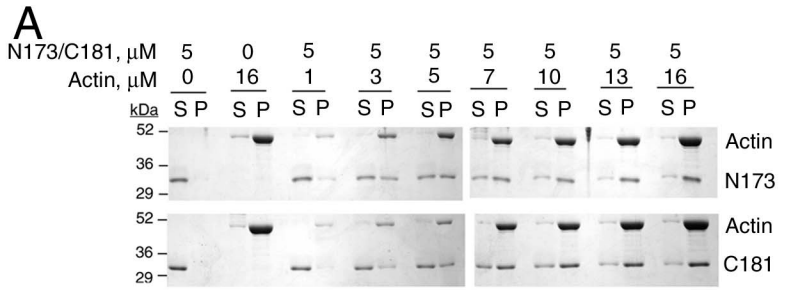

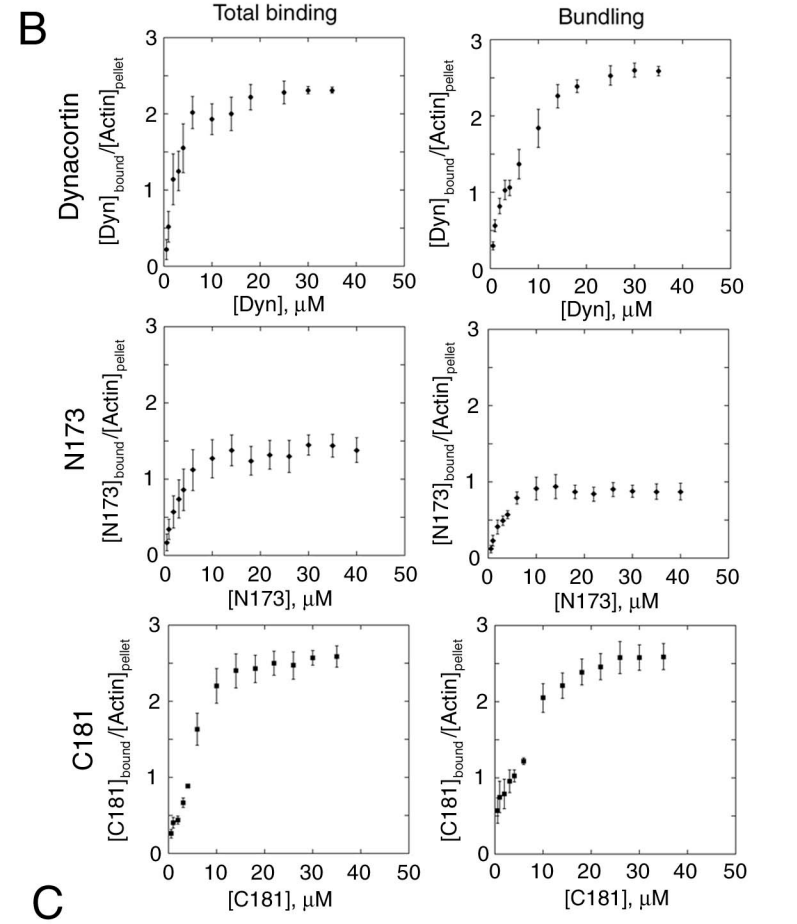

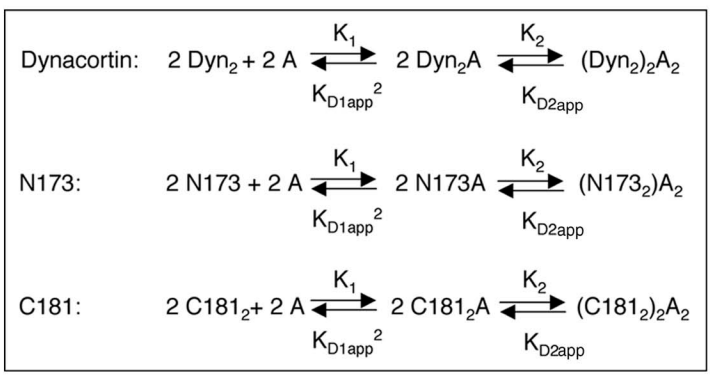

Supplementary Figure 2

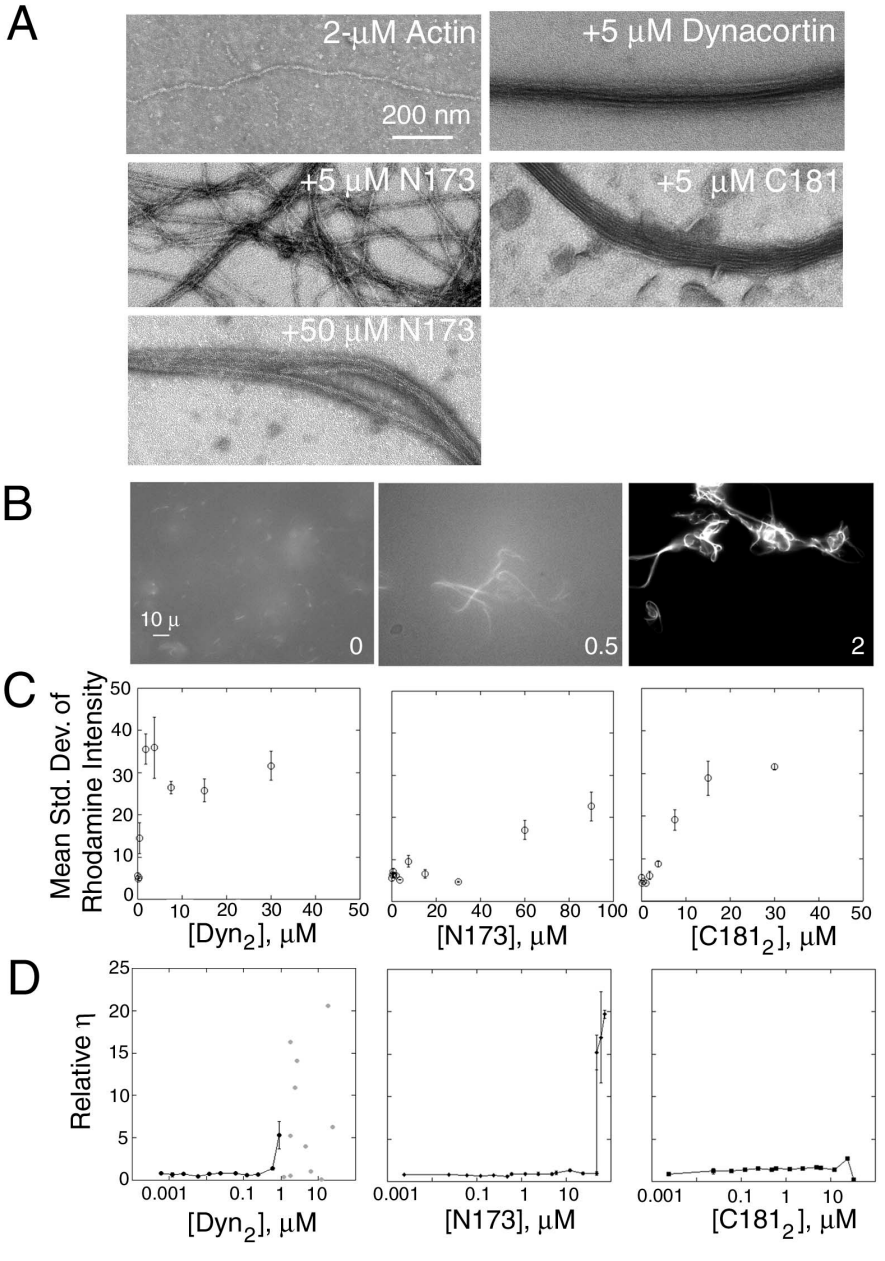

Supplementary Figure 3